Dynamics of Mismatched Base Pairs in DNA†

Christopher R. Guest,‡ Remo A. Hochstrasser,‡ Lawrence C. Sowers,§ and David P. Millar*,‡

Department of Molecular Biology, Research Institute of Scripps Clinic, La Jolla, California 92037, and Division of Pediatrics, City of Hope National Medical Center, Duarte, California 91010

Received July 10, 1990; Revised Manuscript Received December 12, 1990

ABSTRACT: The structural dynamics of mismatched base pairs in duplex DNA have been studied by time-resolved fluorescence anisotropy decay measurements on a series of duplex oligodeoxynucleotides of the general type d[CGG(AP)GGC]·d[GCCXCCG], where AP is the fluorescent adenine analogue 2-aminopurine and X = T, A, G, or C. The anisotropy decay is caused by internal rotations of AP within the duplex, which occur on the picosecond time scale, and by overall rotational diffusion of the duplex. The correlation time and angular range of internal rotation of AP vary among the series of AP·X mismatches, showing that the native DNA bases differ in their ability to influence the motion of AP. These differences are correlated with the strength of base-pairing interactions in the various AP·X mismatches. The interactions are strongest with X = T or C. The ability to discern differences in the strength of base-pairing interactions at a specific site in DNA by observing their effect on the dynamics of base motion is a novel aspect of the present study. The extent of AP stacking within the duplex is also determined in this study since it influences the excited-state quenching of AP. AP is thus shown to be extrahelical in the AP·G mismatch. The association state of the AP-containing oligodeoxynucleotide strand is determined from the temperature-dependent tumbling correlation time. An oligodeoxynucleotide triplex is formed with a particular base sequence in a pH-dependent manner.

Genetic mutations can occur when noncomplementary bases are incorporated into DNA as a result of replication errors or recombination between homologous, but not identical, base sequences. Mismatched bases in DNA are recognized and excised by DNA polymerases having proofreading activities or by postreplicative repair systems (Modrich, 1987). Many combinations of mismatched base pairs can be accommodated within double-helical DNA, and it is found that these are repaired with differing efficiency (Dohet et al., 1985; Kramer et al., 1985; Fersht et al., 1982; White et al., 1985; Wagner et al., 1984). Since mismatch recognition in DNA is not understood at the molecular level, it is useful to characterize the structure and dynamics of various mismatched base pairs in DNA and to determine their effect on the structure of the double helix.

The structures of several mismatched base pairs in DNA have been determined by X-ray crystallography (Kennard, 1986; Brown et al., 1986; Hunter et al., 1986) and nuclear magnetic resonance (NMR)[1] methods (Sowers et al., 1986; Fazakerly et al., 1986, 1987; Patel et al., 1984). However, much less is known about the dynamic properties of mismatched bases in DNA and the possible role of dynamics in mismatch recognition. The bases in DNA move rapidly within the double helix as a result of thermally driven structural fluctuations in solution. Since the base motion occurs within a multidimensional potential well that is determined by a combination of base-stacking and base-pairing forces, the motion of a mismatched base in DNA should be different from that of a matched base pair, and this may influence the interaction of the mismatched base with a repair enzyme. Time-resolved fluorescence anisotropy decay of a fluorescent base (Fleming, 1986; Graslund et al., 1987) is a suitable technique for directly observing the base motion in DNA, which occurs in solution on the picosecond time scale.

We have used the time-resolved fluorescence anisotropy decay of the adenine analogue 2-aminopurine (AP)[1] to examine the base motion within a series of AP·X mismatches in duplex DNA, where X = T, A, G, and C. AP has a high intrinsic fluorescence and can be used as a site-specific fluorescent probe in DNA (Graslund et al., 1987). AP is also nonperturbing as a probe since it can base pair with thymine in a Watson–Crick geometry (Sowers et al., 1986). The dynamics of the AP·T base pair have been previously investigated by NMR, fluorescence, and simulation methods (Nordlund et al., 1989), but little data are available on the dynamics of the other AP-containing base pairs.

In the present study, AP is incorporated at a specific site in a duplex oligodeoxynucleotide and paired with each of the native DNA bases. We present three types of experimental data: (i) Amplitude and correlation time for internal rotation of AP within the DNA double helix. These are influenced by the base-pairing forces acting on AP in the AP·X mismatch and are of the greatest interest in this study. The dynamic properties of different mismatched base pairs in DNA have not been compared before. (ii) Tumbling correlation times. These provide information on the association state of the oligodeoxynucleotide strands. (iii) Emission lifetimes. These report on the excited-state quenching of AP, which is influenced by the stacking of AP within the oligodeoxynucleotide. By combining these different types of information, it is possible to compare the dynamics of various mismatched base pairs in DNA and to assess their effect on the structure of the DNA.

We find that the dynamics of AP motion are not the same in each of the AP·X mismatches and that the native DNA bases differ in their ability to influence the motion of AP. The AP motion is strongly influenced by X = T and C, which

† Supported by a grant from the Swiss National Science Foundation (to R.A.H.) and NIH Grant NIGMS GM41336 (to L.C.S.).

* Address correspondence to this author.
‡ Research Institute of Scripps Clinic.
§ City of Hope National Medical Center.

[1] Abbreviations: AP, 2-aminopurine; NMR, nuclear magnetic resonance.

0006-2960/91/0430-3271$02.50/0

5' C-G-G-AP-G-G-C (I)
3' G-C-C-X-C-C-G (II)

X = T, A, G or C.

FIGURE 1: Oligodeoxynucleotide strands used in the present study. AP is 2-aminopurine. The AP-containing strand is designated strand I.

implies that the base-pairing forces between AP and X are strong in these cases. These observations are pertinent to the ability to AP to form certain stable mispairs in DNA and, possibly, to the molecular basis of mispair recognition by repair enzymes. A preliminary account of part of this work has appeared elsewhere (Millar & Sowers, 1990).

Materials and Methods

Oligodeoxynucleotide Synthesis. The oligodeoxynucleotide strands depicted in Figure 1 were synthesized by the phosphotriester method as described previously (Eritja et al., 1986). The AP-containing strand is referred to as strand I. The central base in strand II is either T, A, G, or C. The strands are dissolved in a buffer containing 50 mM Tris-HCl, pH 7.4, and 0.15 M NaCl and mixed in a 1:1 ratio. The strand concentration is 50 μM. The sample with X = C in strand II was also prepared at pH 8.5.

Steady-State Spectroscopy. The absorption spectra of the oligodeoxynucleotides samples were measured on a Shimdazu Model UV2100U spectrophotometer with a band-pass of 4 nm. The sample conditions were as noted in the preceding section except that the oligonucleotide concentration was 5 μM.

Steady-state fluorescence excitation and emission spectra of the oligodeoxynucleotide samples were measured on a Shimadzu Model RF5000U spectrofluorometer. The sample conditions were as noted in the preceding section. The emission spectrum was recorded with an excitation wavelength of 320 nm, and the excitation spectrum was recorded with the emission observed at 380 nm. The spectral band-pass was 5 nm for both excitation and emission.

Time-Resolved Fluorescence Measurements. The samples were contained in a quartz cuvette placed inside a temperature-controlled housing and were excited at 317 nm with the frequency-doubled output of a synchronously mode-locked and cavity-dumped dye laser (Coherent 702). The DCM laser dye was pumped by a mode-locked argon ion laser (Coherent Innova 100). The repetition rate of the dye laser output was 1.87 MHz, and the pulse duration was 5 ps, as determined by background-free second harmonic autocorrelation. The fluorescence from the samples was collected at right angles to the excitation beam, collimated with a lens, and passed through a sheet polarizer before being focused onto the entrance slit of a 10-cm focal length single-grating monochromator (JY H-10). The polarizer could be oriented parallel, perpendicular, or at 54.7° to the vertical polarization direction of the excitation light with a motor-driven rotary stage under computer control. The monochromator was set to 410 nm, and the band-pass was 4 nm. A microchannel plate photomultiplier (MCP, Hamamatsu R2809U-01) placed at the exit slit was used to detect the fluorescence. The single-photon pulses at the output of the MCP were amplified by 20 dB in a 4-GHz bandwidth amplifier (Mini Circuits Z1042-J) and used to trigger a constant fraction discriminator (CFD, Tennelec 455). The CFD output was sent to the START input of a time-to-amplitude convertor (TAC, Ortec 454). An electrical pulse was derived from a photodiode viewing a portion of the excitation beam and processed by a second CFD (Ortec 583) and was then delayed by 50 ns and sent to the STOP input of the TAC. The TAC output was processed in a pulse height analyzer (PHA, Norland 5150), thereby producing a histogram of photon detection times relative to the excitation pulse. The PHA was operated under remote control by a computer (Masscomp 5400), which was also used for data storage and analysis and control of the emission polarizer direction.

The isotropic emission decay of the samples was measured with the emission polarizer set at 54.7° to the vertical direction and was accumulated until at least 10 000 counts had been collected in the peak channel. The time-dependent emission depolarization was measured by accumulating two separate decay curves, one obtained with the emission polarizer set in the vertical direction and the other set in the horizontal direction. The polarizer was switched between these directions every 15 s, and the two curves were accumulated in separate halves of the PHA memory.

The instrument response function of the system was obtained by scattering the excitation light with a dilute solution of nondairy coffee creamer. The FWHM of the response was typically in the range 45–50 ps.

Data Analysis. The emission lifetimes of AP were determined by analyzing the isotropic decay curve:

$$I(t) = g(t) \otimes K(t) \tag{1}$$

where $g(t)$ is the instrument response function, $K(t)$ describes the decay of the ideal emission intensity, and $\otimes$ denotes convolution of two functions. It was assumed that $K(t)$ could be represented by a multiexponential model:

$$K(t) = \sum_{j=1}^{N} \alpha_j \exp(-t/\tau_j) \tag{2}$$

where α_j is the fractional amplitude associated with the lifetime τ_j. Equations 1 and 2 were fitted to the isotropic decay curve by adjusting N, $\{\alpha_j\}$, and $\{\tau_j\}$ using a nonlinear least-squares method (Bevington, 1969). The numerical evaluation of the convolution integral was facilitated by the use of recursion relations (Grinvald & Steinberg, 1974). The quality of the fit was judged by the reduced χ^2 value, χ_r^2, and by inspection of the weighted residuals (Bevington, 1969).

The time-dependent emission depolarization data were analyzed with the equations:

$$I_{\parallel}(t) = g(t) \otimes \{[1 + 2r(t)]K(t)\} \tag{3a}$$

$$I_{\perp}(t) = g(t) \otimes \{[1 - r(t)]K(t)\} \tag{3b}$$

where $I\|(t)$ and $I_{\perp}(t)$ are the time-resolved intensities of the parallel and perpendicular polarization components of the emission, respectively, and $r(t)$ is the time-dependent emission anisotropy. It was assumed that $r(t)$ could be represented by a multiexponential model:

$$r(t) = \sum_{k=1}^{M} r_{0k} \exp(-t/\tau_{rk}) \tag{4}$$

where r_{0k} is the limiting anisotropy (at time zero) associated with the anisotropy decay time τ_{rk}. The parameters appearing in $K(t)$ were determined from the isotropic decay, as noted above, and were kept constant in the analysis of the depolarization data. Equations 3a, 3b, and 4 were fitted to the two polarized decay curves by adjusting M, $\{r_{0k}\}$, and $\{\tau_{rk}\}$. The quality of the fit was judged as described above.

An implicit assumption of the analysis of the time-dependent depolarization is that each lifetime component in eq 2 is associated with each anisotropy decay component in eq 4. That is, all the cross-terms appearing in eq 3a and 3b are included in the analysis. This assumption is correct if each emitting state of AP undergoes the same internal and overall motion. This assumption is physically reasonable.

Table I: Fluorescence Lifetime Analysis[a]

X[b]	T (°C) (±0.5)	τ_1 (ps) (±5)	τ_2 (ps) (±15)	τ_3 (ns) (±0.05)	τ_4 (ns) (±0.10)	α_1 (±0.010)	α_2 (±0.010)	α_3 (±0.005)	α_4 (±0.005)	χ_r^2
T	40	57	434	2.07	7.27	0.546	0.211	0.181	0.062	1.06
	30	50	438	2.13	7.84	0.586	0.195	0.145	0.074	1.18
	20	44	365	2.06	8.26	0.569	0.214	0.134	0.083	1.04
	10	43	362	2.01	8.55	0.599	0.210	0.115	0.076	1.17
	4	47	379	2.03	8.84	0.585	0.212	0.120	0.083	1.28
G	40	55	404	2.02	7.34	0.493	0.281	0.157	0.069	1.20
	30	58	415	2.10	7.80	0.486	0.294	0.137	0.083	1.20
	20	70	459	1.91	8.35	0.456	0.343	0.121	0.080	1.04
	10	67	484	1.80	8.79	0.476	0.312	0.128	0.084	1.10
	4	71	466	1.66	9.00	0.472	0.290	0.154	0.084	1.17
A	40	55	414	2.05	6.97	0.560	0.228	0.153	0.059	1.08
	30	47	379	2.03	7.34	0.641	0.202	0.100	0.057	1.10
	20	44	392	2.04	8.09	0.681	0.190	0.075	0.054	1.02
	10	44	391	1.89	8.50	0.728	0.162	0.065	0.045	1.06
	4	46	401	1.76	8.62	0.746	0.148	0.064	0.042	1.15
C	40	31	355	1.84	6.28	0.597	0.199	0.145	0.059	1.08
	30	30	354	1.94	7.00	0.665	0.172	0.100	0.063	1.10
	20	48	394	1.94	7.72	0.630	0.200	0.095	0.075	1.02
	10	48	394	1.92	8.37	0.732	0.139	0.071	0.058	1.00
	4	30	296	1.64	8.37	0.749	0.141	0.063	0.047	1.07
C[c]	40	45	427	1.82	6.27	0.574	0.217	0.162	0.047	1.12
	30	51	443	1.97	6.62	0.583	0.194	0.158	0.065	1.14
	20	38	375	1.94	6.95	0.648	0.160	0.125	0.067	1.10
	10	48	417	2.20	7.91	0.752	0.114	0.077	0.057	1.06
	4	35	330	1.97	8.05	0.776	0.113	0.059	0.052	1.19

[a] λ_{ex} = 317 nm, λ_{cm} = 410 nm. pH 7.4 unless otherwise indicated. [b] X is defined in Figure 1. [c] pH 8.5.

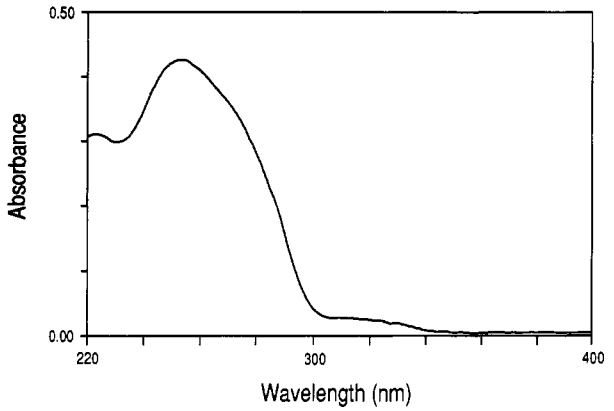

FIGURE 2: Absorption spectrum of 5 μM d[CGG(AP)GGC]·d-[GCCTCCG] in 50 mM Tris-HCl, pH 7.4, and 0.15 M NaCl at 20 °C.

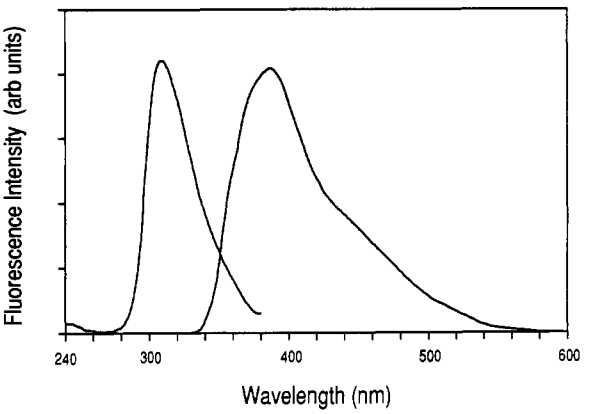

FIGURE 3: Steady-state fluorescence excitation (at left) and emission (at right) spectra of 50 μM d[CGG(AP)GGC]·d[GCCTCCG] in 50 mM Tris-HCl, pH 7.4, and 0.15 M NaCl at 20 °C. In the excitation spectrum, the emission is observed at 380 nm, while in the emission spectrum the excitation wavelength is 320 nm. The band-pass is 5 nm for both excitation and emission.

RESULTS

Absorption and Emission Spectra. The absorption spectrum of the oligodeoxynucleotide sample with X = T at 20 °C is shown in Figure 2. The spectrum exhibits the expected absorption band at 260 nm due to the native DNA bases and a shoulder centered at 320 nm due to absorption by AP. The absorption spectra of the samples with X = A, G, and C are very similar to the spectrum shown in Figure 2. The spectra are similar to those previously reported for these oligodeoxynucleotides (Eritja et al., 1986).

The steady-state fluorescence excitation and emission spectra of the sample with X = T at 20 °C are shown in Figure 3. The excitation spectrum exhibits a peak at 320 nm and is very similar in shape to the AP absorption band seen in the absorption spectrum of this sample (Figure 2). This demonstrates that the emission being observed is specifically due to AP. The emission spectrum exhibits a peak at 380 nm and has an asymmetric shape, with a tail extending to the long-wavelength side of the spectrum.

Emission Lifetimes. The isotropic emission decay of the oligodeoxynucleotides depicted in Figure 1 was measured over the temperature range 4–40 °C at pH 7.4. The sample with X = C in strand II was also investigated at pH 8.5. The lifetime analysis of the isotropic decay curves is shown in Table I. Four lifetime components are required to obtain an adequate fit to the data on all the measured time scales (from 7 to 90 ps/channel). The results in Table I represent weighted averages of data from several time scales and of several duplicate measurements for each set of experimental conditions. The χ_r^2 values are close to 1.0, and there is no evidence of systematic deviations in the weighted residuals.

The isotropic fluorescence decay of the free 2-aminopurine nucleoside in 50 mM Tris-HCl buffer, pH 7.4, was measured for comparison with the results in Table I. The decay is monoexponential with a fluorescence lifetime of 10.43 ± 0.06 ns at 20 °C.

At 40 °C, the emission decay behavior of AP in the oligodeoxynucleotide samples is independent of the base X contained in strand II (Table I). At this temperature, the oligodeoxynucleotides are present in single-strand form, and the AP base consequently has the same local environment in each of the samples. At lower temperatures, however, the results

Table II: Anisotropy Decay Parameters[a]

X[b]	T (°C) (±0.5)	τ_{r1} (ps) (±15)	τ_{r2} (ns) (±0.07)	r_{01} (±0.015)	r_{02} (±0.015)	r_0 (±0.030)	χ_r^2
T	40	60	0.50	0.210	0.127	0.337	1.18
	30	73	0.65	0.229	0.127	0.356	1.20
	20	85	0.80	0.227	0.117	0.344	1.17
	10	100	1.10	0.235	0.106	0.341	1.22
	4	124	1.70	0.249	0.099	0.348	1.14
G	40	60	0.54	0.204	0.138	0.342	1.09
	30	65	0.70	0.196	0.138	0.334	1.14
	20	69	1.30	0.203	0.128	0.331	1.23
	10	72	1.62	0.204	0.129	0.333	1.23
	4	83	1.91	0.206	0.130	0.336	1.29
A	40	60	0.54	0.201	0.144	0.345	1.22
	30	68	0.65	0.211	0.143	0.354	1.05
	20	71	0.84	0.205	0.142	0.347	1.19
	10	75	1.12	0.218	0.143	0.361	1.33
	4	89	1.73	0.212	0.143	0.355	1.23
C	40	67	0.67	0.211	0.147	0.358	1.22
	30	98	1.19	0.210	0.139	0.349	1.33
	20	101	1.97	0.204	0.138	0.342	1.35
	10	101	2.73	0.202	0.142	0.344	1.38
	4	92	2.81	0.191	0.147	0.338	1.19
C[c]	40	62	0.53	0.190	0.160	0.350	1.24
	30	79	0.64	0.206	0.159	0.365	1.25
	20	90	0.78	0.216	0.161	0.377	1.08
	10	101	1.12	0.171	0.169	0.340	1.31
	4	109	1.77	0.189	0.167	0.356	1.19

[a] λ_{ex} = 317 nm, λ_{em} = 410 nm. pH 7.4 unless otherwise indicated. [b] X is defined in Figure 1. [c] pH 8.5.

in Table I indicate that the AP decay exhibits some dependence on the identity of the base X contained in strand II. The following observations were made: (i) The extent of AP quenching at 4 °C, as judged by the amplitude α_1 of the shortest lifetime, decreases in the order X = C (pH 8.5), C (pH 7.4), A, T, G. The same order applies if the quenching is judged by the magnitude of τ_1. (ii) The extent of quenching increases with decreasing temperature in the samples with X = A or C (both pH values). In the sample with X = T, the quenching remains approximately constant over the same temperature range, whereas in the sample with X = G the quenching decreases slightly with decreasing temperature. Although the differences noted here are small, they are larger than the error ranges associated with each of the decay parameters.

These observations demonstrate that the emission decay behavior of AP is quite similar in the samples with X = T, A, or C contained in strand II. However, with X = G in strand II, the decay behavior is different, especially at low temperature.

Emission Anisotropy Decay. The best fit to the emission depolarization data is obtained when the time-dependent anisotropy is represented by eq 4 with two decay components. Typical time-dependent depolarization data are shown in Figure 4 together with the best fit. The anisotropy decay times and their associated amplitudes are presented in Table II, along with the reduced χ^2 values for the best fit. The best-fit parameters do not vary with the time scale of the measurement (from 7 to 90 ps/channel). The data in Table II are weighted averages of several different determinations for each sample and temperature.

The longer anisotropy decay time, τ_{r2}, is plotted versus η/T in Figure 5, where η is the solution viscosity at each temperature T as determined from standard tables (CRC Handbook of Chemistry and Physics, 71st ed., 1990). The samples with X = T, A, and C (pH 8.5) exhibit a similar dependence of τ_{r2} on η/T over the entire temperature range. In these samples, τ_{r2} varies linearly with η/T between 20 and 40 °C. The heavy solid line in Figure 5 extrapolates the linear dependence across the entire temperature range. At temperatures below 20 °C, τ_{r2} is larger than expected from the linear extrapolation and varies more strongly with temperature.

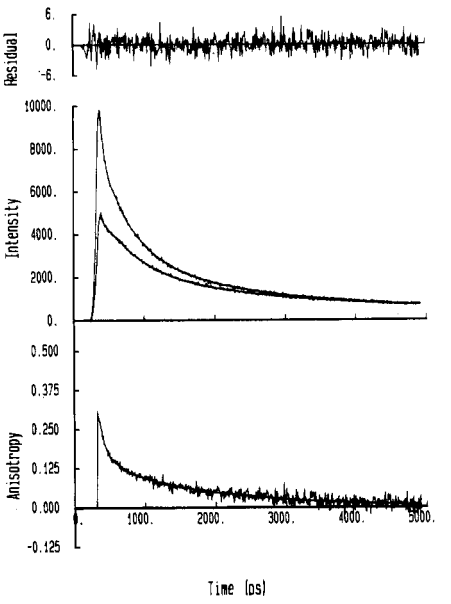

FIGURE 4: Time-resolved emission depolarization of d[CGG(AP)GGC]·d[GCCGCCG] in 50 mM Tris-HCl, pH 7.4, and 0.15 M NaCl at 4 °C. The center panel shows the polarized emission intensities $I_{\parallel}(t)$ (upper curve) and $I_{\perp}(t)$ (lower curve). The time-dependent emission anisotropy is shown in the lower panel. The smooth lines are best-fit curves generated as described in the text. The upper panel shows the weighted deviation between the experimental difference curve, $I_{\parallel}(t) - I_{\perp}(t)$, and the best-fit difference curve.

The samples with X = G or C (pH 7.4) exhibit larger values of τ_{r2} than the other samples at most temperatures (Table II and Figure 5).

The short anisotropy decay time τ_{r1} is attributed to an internal motion of the AP base since it is too short to be due to overall motion of a seven-base oligodeoxynucleotide. The internal motion is restricted in amplitude since it does not cause complete depolarization of the fluorescence.

The anisotropy decay behavior is analyzed with a phenomenological model of restricted internal rotation of AP and

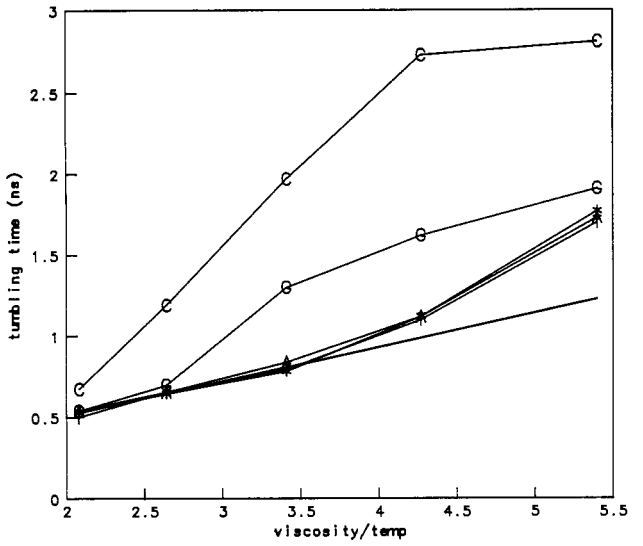

FIGURE 5: Tumbling correlation time of d[CGG(AP)GGC]·d-[GCCXCCG] versus η/T, where η and T are the solution viscosity and temperature, respectively. The (η/T) axis is labeled in units of 10^{-10} kg m s^{-1} K^{-1}. The data points for X = T, A, G, and C at pH 7.4 are marked with the corresponding letters. The data points for X = C at pH 8.5 are marked with asterisks. The heavy solid line shows the expected behavior for a seven-base single-strand oligodeoxynucleotide obtained by extrapolating the data at temperatures above 20 °C across the entire temperature range. See text for details.

overall tumbling of the oligonucleotide (Lipari & Szabo, 1980). The anisotropy decay is represented by

$$r(t) = r_0[S^2 + (1 - S^2)\exp(-t/\tau_i)]\exp(-t/\tau_T) \quad (5)$$

where τ_i is the correlation time for internal motion, τ_T is the correlation time for overall tumbling, and S is the generalized order parameter. This equation assumes that internal rotation and overall rotation are independent. The model parameters are related to the anisotropy decay parameters defined in eq 4:

$$\tau_i = (\tau_{r1}^{-1} - \tau_{r2}^{-1})^{-1} \quad (6)$$

$$\tau_T = \tau_{r2} \quad (7)$$

$$S = [r_{01}/(r_{01} + r_{02})]^{1/2} \quad (8)$$

The internal correlation time τ_i is presented in Table III and plotted in Arrhenius form in Figure 6. It is evident that the temperature dependence of this correlation time depends on the identity of the base X contained in strand II and on the solution pH in the case of X = C. The order parameter is also presented in Table III. This is a model-independent measure of the order in the equilibrium orientational distribution of the AP bases (Lipari & Szabo, 1980). The angular range of AP internal motion is related to the order parameter by assuming that the restricted motion can be modeled as free diffusion within a cone (Kinosita et al., 1977). The cone semiangle is given by

$$\theta_0 = \cos^{-1}\{(1/2)[(1 + 8S)^{1/2} - 1]\} \quad (9)$$

The θ_0 values are also presented in Table III. These values are independent of temperature and are the same in the samples with X = A, G, and C (both pH values). However, θ_0 varies with temperature in the sample with X = T.

Table III: Correlation Time, Order Parameter, and Cone Angle for Restricted Motion of 2-Aminopurine[a]

X[b]	T (°C) (±0.5)	τ_i (ps) (±15)	S (±0.070)	θ_0 (deg) (±3)
T	40	68	0.614	44
	30	82	0.597	45
	20	95	0.583	46
	10	110	0.558	48
	4	135	0.533	50
G	40	68	0.635	43
	30	72	0.643	42
	20	73	0.622	44
	10	75	0.622	44
	4	87	0.622	44
A	40	68	0.646	42
	30	76	0.636	43
	20	78	0.640	43
	10	80	0.629	43
	4	94	0.635	43
C	40	74	0.641	42
	30	107	0.631	43
	20	106	0.635	43
	10	105	0.642	42
	4	95	0.659	41
C[c]	40	70	0.676	40
	30	90	0.660	41
	20	102	0.653	42
	10	111	0.705	38
	4	116	0.685	39

[a] pH 7.4 unless otherwise indicated. [b] X is defined in Figure 1. [c] pH 8.5.

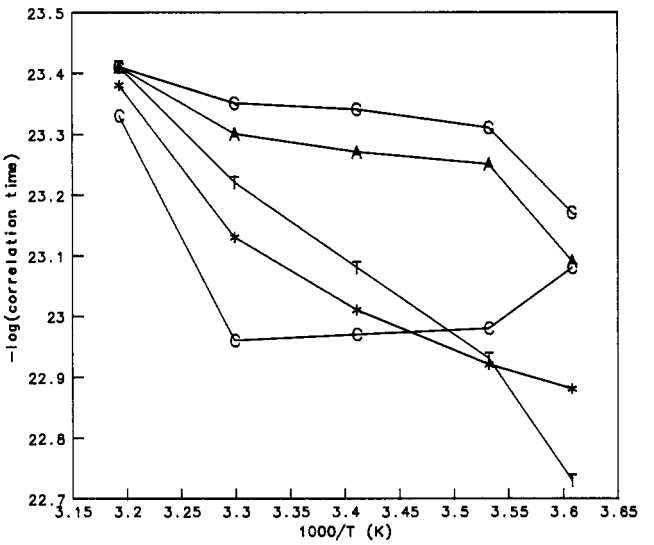

FIGURE 6: Temperature dependence of the internal motion correlation time of AP in d[CGG(AP)GGC]·d[GCCXCCG] plotted in Arrhenius form. The data points for X = T, A, G, and C at pH 7.4 are marked with the corresponding letters. The data points for X = C at pH 8.5 are marked with asterisks. The lines are drawn to connect the data points.

Discussion

Emission Kinetics of AP in an Oligodeoxynucleotide. The fluorescence decay of the AP nucleoside in aqueous solution is monoexponential with a lifetime of 10.43 ns at 20 °C. When the AP nucleoside is incorporated in an oligodeoxynucleotide, the emission intensity is reduced, and there are four decay components instead of one (Table I). The correspondence between the excitation spectrum and the AP absorption band (Figures 2 and 3) demonstrates that the emission is specifically due to AP and hence that all four lifetimes are associated with AP. The spectrum of decay times measured in the present work is similar to that reported by Graslund et al. (1987) for AP contained in a self-complementary oligodeoxynucleotide 10-mer.

The longest lifetime of AP in the oligonucleotide (τ_4) is similar to the lifetime of the free AP nucleoside and thus probably represents the fluorescence emission from AP bases

that are not electronically quenched in the oligodeoxynucleotide strand. The contribution of this component to the initial emission intensity is very small in all the samples and is essentially independent of temperature. This component may represent a small subset of the AP bases that are not stacked with their neighboring bases and are therefore not quenched upon excitation. However, this component contributes about 50% of the integrated emission intensity because of its long lifetime.

The three shorter lifetime components of AP are present at all temperatures in each of the oligonucleotide samples and in general depend only weakly on the identity of the base X contained in strand II. These components are therefore due to emitting states that arise primarily from interactions of AP with the bases contained within the same strand (strand I). Since AP is very similar in structure to the purine bases occurring naturally in DNA, it should stack with its neighboring bases on strand I. The interaction of an electronically excited AP base with the nearest-neighbor bases should be quite strong due to the parallel orientation and close proximity established by the base-stacking interactions in the electronic ground state. These excited-state interactions could involve electronic energy transfer, exciplex formation and charge transfer. It is reasonable to suppose that the shortest lifetime component is associated with the fluorescence emission of AP bases that are stacked with their neighboring bases. Since more than 50% of the initial emission intensity is associated with this component, it represents the major species present, which is consistent with it being due to the stacked form of the AP base. However, this component makes a negligible contribution to the integrated emission intensity because of its very short lifetime.

The lifetimes τ_2 and τ_3 are similar to the reported lifetimes of base excimer fluorescence (τ_2) and phosphorescence (τ_3) emissions from synthetic homopolynucleotides (Ballini et al., 1982). It is possible that the emissions associated with τ_2 and τ_3 are due to the fluorescence and phosphorescence, respectively, of an exciplex of AP and a nearest-neighbor guanine base on strand I (Figure 1). This would also explain the asymmetric band shape of the emission spectrum (Figure 3), since the spectra of base exciplex emissions are red-shifted relative to the monomer fluorescence in nucleic acids (Morgan & Daniels, 1980).

Excited-State Quenching of AP. The shortest emission lifetime (τ_1) and its associated amplitude (α_1) reflect the extent of excited-state quenching of AP monomers in the oligodeoxynucleotides. As noted above, this quenching is dominated by interactions occurring within the AP-containing strand. However, at 4 °C, the oligodeoxynucleotide strands are present in associated form, and the extent of AP quenching varies somewhat according to the identity of the base X opposite AP. It is argued later, on the basis of the observed tumbling correlation time and its dependence on temperature, that the strands are present at 4 °C as regular DNA duplexes in the samples with X = T, A, or C (pH 8.5). The extent of AP quenching at 4 °C is the same in the latter two samples and is greater than in the single-strand state at 40 °C. This could mean that the bases on strand I are better stacked at low temperature in these samples, or it may indicate that in the duplex state there are additional interactions occurring between AP and the bases on strand II. However, in the sample with X = T, the extent of AP quenching is approximately equal in the duplex state and the single-strand state. This observation supports the conclusion that the extent of AP quenching is determined by the degree of base stacking within strand I, which is less in the duplex containing X = T than in the duplexes containing X = A or C, possibly because the base-pairing forces acting between AP and T (Sowers et al., 1986) are sufficiently strong to prevent the AP base from adopting the most highly stacked configuration with its nearest neighbors on strand I. The AP·T base pair is found to be the most stable on the basis of the relative T_m values of these duplexes (Eritja et al., 1986). Also, it appears that the H-bonding interactions involved in base-pairing between AP and T (Sowers et al., 1986) do not cause additional excited-state quenching of AP.

The sample with X = C at pH 7.4 is proposed to contain a large fraction of a triplex association state at 4 °C, on the basis of the tumbling correlation times discussed later. The extent of AP quenching is greater in this associated state than in the single-strand state, indicating that AP is better stacked with its neighbors.

Tumbling Correlation Time of AP-Containing Oligodeoxynucleotides. The correlation time for overall tumbling of a molecule in solution can be determined experimentally from the decay of the time-resolved fluorescence anisotropy (Fleming, 1986). The anisotropy decay of the oligodeoxynucleotides containing an AP base probe exhibits two decay times. The longer decay time (τ_{r2}) is attributed to overall tumbling according to eq 4–7. At 40 °C, all the oligodeoxynucleotide samples have essentially the same tumbling time, independent of the base X contained in strand II. At this temperature, the AP-containing strand is present in single-strand form in all the samples, and the tumbling time is consequently the same in each case.

Between 20 and 40 °C, the tumbling time varies linearly with η/T in the samples with X = T, A, and C (pH 8.5). Such a dependence is expected for overall tumbling according to the Stokes–Einstein equation (Fleming, 1986). The slope of the linear dependence is proportional to the molecular volume, which is apparently constant over the temperature range from 20 to 40 °C in these samples. The observed slope is consistent with the expected tumbling behavior of a prolate ellipsoid of length 24 Å and diameter 16 Å, calculated from a rotational diffusion model (Fleming, 1986). These dimensions are reasonable for a seven-base single-strand oligodeoxynucleotide and suggest that the samples with X = T, A, and C (pH 8.5) are largely in single-strand form between 20 and 40 °C.

The expected η/T dependence of the tumbling time of the single-strand oligonucleotide over the entire temperature range is shown by the heavy solid line in Figure 5. It is apparent that below 20 °C, the samples with X = T, A, and C (pH 8.5) have tumbling times which exceed the value expected for a single strand, indicating that strand I associates with strand II to form a species with a larger molecular volume. Since the tumbling time of these samples is very similar, the same species is apparently formed in each case. Figure 5 also shows that τ_{r2} depends more strongly on η/T below 20 °C. In fact, the slope of the linear dependence increases by about a factor of 2 below 20 °C, suggesting that the strands are associating to form an oligodeoxynucleotide duplex. The samples with X = T, A, and C (pH 8.5) in strand II appear to be largely in duplex form below 20 °C.

The association of the oligodeoxynucleotide strands studied here has been previously reported based on the temperature dependence of the UV absorption spectra (Eritja et al., 1986). The melting transitions are very broad and extend from 10 to 45 °C. The melting temperature T_m was determined by locating the inflection point in the melting curve by calculating its first and second derivatives with respect to temperature.

The T_m values reported for the same solvent conditions used in the present study (pH 7.4) are 31.4 °C for X = T, 28.0 °C for X = A, and 24.9 °C for X = C.

The tumbling time of an AP-containing oligonucleotide strand accurately reflects the state of association of the strand and therefore provides complementary information to that obtained from an optical melting study.

AP Is Extrahelical in the AP·G Mismatch. The sample with X = G in strand II tumbles more slowly than expected (Figure 5). This sample should contain the least proportion of associated strands, since it has the lowest T_m value (20.4 °C; Eritja et al., 1986), and yet it exhibits a larger tumbling time than the most stable duplex (X = T) over most of the temperature range. This suggests that when strand II contains X = G, it associates with strand I to form a structure that has a different shape than a regular DNA duplex. The excited-state quenching of AP in this sample is also different from the other samples (Table I). In this sample, the AP quenching is reduced as the temperature is lowered, which is evident in the increase in τ_1 and τ_2 under these conditions (Table I). AP is therefore less quenched in the associated state than in the single-strand state. However, with X = T, A, or C in strand II, the quenching is greater in the associated state and increases as the temperature is lowered (Table I). Since the excited-state quenching of AP is most likely caused by electronic interactions of AP and its neighboring bases, which are facilitated by stacking of the bases, this observation suggests that AP is not base-stacked in the associated species which forms at low temperature when strand II contains X = G. The associated state may involve a "looped-out" structure in which the AP base is unstacked and extrahelical. This structure will have a larger effective radius than a regular duplex and will tumble more slowly, as observed below 20 °C (Figure 5). Another possibility is that the duplex is bent at the AP site because of the extrahelical conformation, which will also result in slower tumbling compared to a regular duplex.

The temperature dependence of the near-UV absorption spectrum of these oligodeoxynucleotides also suggests that AP is unstacked in the AP·G mismatch (Eritja et al., 1986). In the samples with X = T, A, or C, the AP absorption at 330 nm exhibits a cooperative hypochromic shift at a transition temperature close to that of the cooperative hyperchromic shift observed at 275 nm, indicating that the AP base is annealed within the helix in these samples at low temperature. However, with X = G in strand II, there is no cooperative transition apparent in the 330-nm absorption, suggesting that the AP base is not stacked within the helix (Eritja et al., 1986).

An A·G mismatch in a duplex oligonucleotide has been studied by NMR spectroscopy (Fazakerley et al., 1986). A "looped-out" structure was present in which the A and G bases were extrahelical. The A·G mismatch thus appears to behave similarly to the AP·G mismatch studied in the present work, although only the AP base can be observed by fluorescence and it is unknown whether the G base is also extrahelical in the AP·G mismatch.

Triple-Helix Formation. The sample with X = C in strand II exhibits slower tumbling than all the other samples over most of the temperature range at pH 7.4 (Figure 5). However, at pH 8.5, the tumbling time is significantly shorter than at pH 7.4 and is nearly identical with the samples with X = T and A over the entire temperature range (Figure 5). These observations suggest that when strand II contains X = C, it associates with strand I to form a duplex under basic pH conditions, but that a larger species is formed at neutral pH. Strand II contains a dC_5 sequence when X = C (Figure 1). Repeated homopyrimidine sequences have a propensity for triplex formation with repeated homopurine sequences, in which a second pyrimidine strand is Hoogsten base-paired in the major groove of the pyrimidine/purine duplex to form a DNA triple helix (Felsenfeld et al., 1957; Moser & Dervan, 1987; Lyamichev et al., 1988). DNA triplexes containing cytosine bases on the pyrimidine strand are observed to be stable at acidic and neutral pH, but are unstable under basic conditions since the Hoogsten pairing requires that the cytosine bases on the third strand be in protonated form (Felsenfeld et al., 1957; Mirkin et al., 1987; Moser & Dervan, 1987; Lyamichev et al., 1988). The apparent pK value for triplex structures involving protonated cytosines is between 7.0 and 7.4 (Povsic & Dervan, 1989; Rajagopal & Feigon, 1989). We suggest that the oligodeoxynucleotide strands shown in Figure 1 with X = C can associate to form a DNA triplex involving a second strand II in which the cytosine bases are in protonated form. Since strands I and II are present in equimolar amounts, no more than half of the AP-containing strands can be bound in triplexes, while the remainder are present as single strands or duplexes. The AP-containing strand is probably present in a mixture of association states, and the observed tumbling time therefore represents an average value for the mixture. The tumbling time of a triplex oligonucleotide is therefore larger than the value given in Table II. The presence of the AP base disrupts the strict homopurine sequence on strand I but does not appear to prevent triplex formation. A measurement of the tumbling time of oligodeoxynucleotides containing an AP fluorescent probe can therefore be used to detect the formation of triple-helical DNA in solution.

Internal Motion Dynamics of AP. The anisotropy decay time τ_{r1} is too fast to represent tumbling of a seven-base oligodeoxynucleotide and is therefore attributed to a restricted rotational motion of AP within the oligodeoxynucleotide strand. The precise nature of this motion cannot be inferred from the fluorescence anisotropy decay. A variety of DNA internal motions such as helical twisting, propeller twisting, base tilting, and base rolling could potentially rotate the emission dipole of AP and contribute to the fluorescence anisotropy decay.

For a single motional process, the internal correlation time appearing in eq 5 is a function not only of the wobbling diffusion coefficient but also of the cone semiangle and the direction of the wobbling axis (Lipari & Szabo, 1980). Thus, a change in τ_i is not necessarily caused by a change in the rate of internal motion. In the present system, where a number of motional processes may contribute to the fluorescence anisotropy decay, the relationship between the apparent internal correlation time and cone angle and the true correlation time and angular range of motion associated with each of the individual dynamic processes will be complex and will depend on a number of microscopic parameters that cannot be determined here. Nevertheless, the fluorescence anisotropy decay of AP provides a direct means of observing very rapid base motions within DNA. Furthermore, the AP base is a site-specific probe, and consequently, the base dynamics in a local region of DNA can be selectively observed.

Effect of Base Pairing on Base Motion. We have exploited the site-specific nature of the AP base probe to examine the influence of base-pairing interactions on base motion in DNA. Each of the four native bases have been placed opposite AP in a duplex or triplex oligodeoxynucleotide, and their effects on the internal motion dynamics of AP have been compared.

The oligodeoxynucleotides with X = T or A in strand II are largely in duplex form below 20 °C. The tumbling times of

these two duplexes are identical, but the dynamics of AP internal motion within the two duplexes are quite different. These differences are reflected in the internal motion correlation time, the angular range of internal motion, and the temperature dependence of both these quantities (Table III and Figure 6). In the sample with X = A, the internal correlation time varies only weakly with temperature, and the angular range of AP motion is independent of temperature. The dynamics of the AP internal motion are therefore essentially the same in the single-strand state and in the duplex containing the AP·A mismatch. We conclude that the local motion of AP is hardly perturbed by the presence of adenine in the AP·A mismatch. However, in the sample with X = T in strand II, the internal correlation time follows an Arrhenius-type temperature dependence with an activation energy of 16 kJ mol^{-1}, and the range of AP internal motion increases substantially as the temperature decreases (Table III and Figure 6). The AP motion is therefore different in the single-strand state compared with the duplex state containing the AP·T mismatch. These dynamic differences indicate that AP undergoes lower frequency motion in the duplex state compared with the single-strand state, suggesting that AP is part of a larger structural unit in the duplex. On the basis of these observations, AP appears to form a stable base pair with thymine which moves as a single unit in the duplex. This is consistent with a molecular dynamics simulation of an AP·T base pair in duplex DNA in which the hydrogen bonds between AP and T are maintained while both bases are in motion (Nordlund et al., 1989).

The structures of the AP·T and AP·A mismatches in the same oligodeoxynucleotide duplexes studied here have been determined by NMR spectroscopy (Sowers et al., 1986; Fazakerley et al., 1987). The AP·T mismatch is found to adopt a normal Watson–Crick structure with two hydrogen bonds between AP and T (Sowers et al., 1986). The AP·A mismatch, on the other hand, appears to adopt a wobble structure with only one hydrogen bond (Fazakerley et al., 1987). The present study of the AP motion in the AP·T and AP·A mismatches provides a different view of the base-pairing interactions. The AP motion is strongly influenced by the presence of thymine in the AP·T mismatch, suggesting that significant interactions occur between the two bases. This is consistent with the formation of two Watson–Crick hydrogen bonds between AP and T. However, the AP motion is hardly influenced by the presence of adenine in the AP·A mismatch, suggesting that the interactions between the two bases is weak. This is consistent with the one hydrogen bond between AP and A suggested by the NMR data. By observing the effect of the opposing base on the motion of AP, information is obtained on the strength of the interactions between the two bases at a specific site in the DNA duplex.

In the AP·G mismatch, the AP base is excluded from the base stack as discussed above. The AP internal motion in this case is faster than in any of the other oligodeoxynucleotides, which is consistent with the absence of base-pairing forces between AP and G in this sample.

pH-Dependent Dynamics of the AP·C Mismatch. The internal motion dynamics of AP in the AP·C pair are different at pH 7.4 compared with pH 8.5 (Table III and Figure 6). At pH 8.5, the temperature dependence of the internal motion correlation time is very similar to the AP·T mismatch. This suggests that significant base-pairing forces are acting between AP and C under these conditions. Sowers et al. (1989) have shown that the AP·C mismatch in the same oligonucleotide studied here exists as a neutral wobble structure at pH 8.6, with two hydrogen bonds between AP and C. According to the present study, the effect of these two hydrogen bonds is to influence the internal motion of AP in a similar fashion to the AP·T base pair, which also has two hydrogen bonds.

However, at pH 7.4, the temperature dependence of the internal motion correlation time is different than that observed at pH 8.5 and is more complicated than in any of the other samples (Figure 6). The correlation time increases as the temperature decreases from 40 to 20 °C, but then decreases as the sample is cooled below 20 °C. This behavior suggests that different forms of the AP·C mismatch are present in a temperature-dependent equilibrium. Since it is unlikely that the wobbling diffusion coefficient will actually increase as the temperature decreases, the apparent decrease of the internal correlation time below 20 °C may reflect the increasing contribution of a form in which either the angular range of motion or the direction of the wobbling axis is different. The two forms could be duplex and triplex association states. Hoogsten-pairing of the additional strand in the triplex state could potentially alter the direction of the wobbling axis of AP and thereby change the observed internal correlation time. The possibility that AP is present in a dynamic equilibrium between different forms at pH 7.4 is supported by the absence of an ^{15}N NMR spectrum in a derivative of this oligodeoxynucleotide in which AP is isotopically enriched in ^{15}N (Sowers et al., 1989). However, at pH 8.6, a single AP species is observed in the ^{15}N spectrum (Sowers et al., 1989).

The base pairing of AP with C is clearly different under neutral as compared to basic pH conditions, and this difference is manifested in the internal motion dynamics of AP.

Conclusions

We have examined the dynamics of the AP·X mismatches in double-helical DNA, where X = T, A, G, and C, by directly observing the AP motion in the picosecond time domain using time-resolved fluorescence anisotropy decay. The AP motion is not the same in each of the mismatched base pairs since the native DNA bases differ in their ability to influence the motion of AP. These differences reflect the strength of the base-pairing interactions between AP and X. These interactions are strongest with X = T or C. The ability to discern differences in the strength of base-pairing interactions at a single site in DNA by observing their effect on base motion is a novel aspect of the present study. The time-resolved fluorescence of AP in an oligodeoxynucleotide also provides information on the association state of the oligonucleotide and the stacking of AP within the oligonucleotide strand, so that some information on the effect of the AP·X mismatch on the structure of DNA has also been obtained.

Our conclusions regarding each of the AP·X mismatches are as follows. *AP·T.* Strands I and II form a duplex below about 20 °C in which AP is stacked within the helix. AP forms a stable base pair with thymine which has different motional characteristics to an unpaired AP base. It is significant in this regard that AP preferentially base pairs with thymine during DNA synthesis, thereby giving rise to the mutagenic properties of AP (Bessman et al., 1974; Clayton et al., 1979). *AP·A.* AP is stacked within a duplex, but the dynamics of AP motion are hardly perturbed by adenine. The base-pairing forces between AP and adenine are much weaker than between AP and thymine. *AP·C.* Strands I and II form a duplex at pH 8.5 with AP stacked within the helix. The AP motion is perturbed and is similar to that in the AP·T mismatch, suggesting that AP also forms a stable base pair with cytosine. This explains why AP can cause A·T ↔ G·C transitions during replication (Watanabe & Goodman, 1981; Mhaskar &

Goodman, 1984). At neutral pH, strands I and II appear to be present in a mixture of association states, probably a duplex state and a triplex state involving a second strand II in which the cytosine bases are in protonated form. The latter state can form as a result of the specific base sequence of strand II in this case. *AP·G*. AP is unstacked and extrahelical, effectively enlarging the radius of the DNA helix or kinking the helix axis. The AP internal motion is not influenced by the guanine base.

Registry No. Strand I·strand II X = T, 105391-24-0; strand I·strand II X = A, 105356-93-2; strand I·strand II X = G, 105356-95-4; strand I·strand II X = C, 125498-80-8; dT, 50-89-5; dA, 958-09-8; dG, 961-07-9; dC, 951-77-9; dAp, 3616-24-8.

REFERENCES

Ballini, J. P., Daniels, M., & Vigny, P. (1982) *J. Lumin. 27*, 389.

Bessman, M. J., Muzycka, N., Goodman, M. F., & Schnaar, R. L. (1974) *J. Mol. Biol. 88*, 409.

Bevington, P. R. (1969) *Data Reduction and Error Analysis for the Physical Sciences*, McGraw-Hill, New York.

Brown, T., Hunter, W. N., Kneale, G., & Kennard, O. (1986) *Proc. Natl. Acad. Sci. U.S.A. 83*, 2402.

Clayton, L. K., Goodman, M. F., Branscomb, E. W., & Galas, D. J. (1979) *J. Biol. Chem. 254*, 1902.

Dohet, C., Wagner, R., & Radman, M. (1985) *Proc. Natl. Acad. Sci. U.S.A. 82*, 503.

Eritja, R., Kaplan, B. E., Mhaskar, D., Sowers, L. C., Petruska, J., & Goodman, M. F. (1986) *Nucleic Acids Res. 14*, 5869.

Fazakerley, G. V., Quignard, E., Woisard, A., Guschlbauer, W., Van der Marel, G. A., Van Boom, J. H., Jones, M., & Radman, M. (1986) *EMBO J. 5*, 3697.

Fazakerley, G. V., Sowers, L. C., Eritja, R., Kaplan, B. E., & Goodman, M. F. (1987) *Biochemistry 26*, 5641.

Felsenfeld, G., Davies, D. R., & Rich, A. (1957) *J. Am. Chem. Soc. 79*, 2023.

Fersht, A. R., Knill-Jones, J. W., & Tsui, W. C. (1982) *J. Mol. Biol. 156*, 37.

Fleming, G. R. (1986) *Chemical Applications of Ultrafast Spectroscopy*, Oxford University Press, Oxford, U.K.

Graslund, A., Claesens, F., McLaughlin, L. W., Lycksell, P.-B., Larsson, U., & Rigler, R. (1987) in *Structure, Dynamics and Function of Biomolecules, Springer Series in Biophysics* (Ehrenberg, A., Rigler, R., Graslund, A., & Nilsson, L., Eds.) Vol. 1, p 201, Springer Verlag, Berlin.

Grinvald, A., & Steinberg, I. Z. (1974) *Anal. Biochem. 59*, 583.

Hunter, W. N., Brown, T., Anand, N. N., & Kennard, O. (1986) *Nature 320*, 552.

Kennard, O. (1986) in *Trends in Nucleic Acids Research* (Lilley, D., & Eckstein, F., Eds.) Springer-Verlag, Heidelberg.

Kinosita, K., Kawato, S., & Ikegami, A. (1977) *Biophys. J. 20*, 289.

Kramer, B., Kramer, W., & Fritz, H. J. (1985) *Cell 38*, 879.

Lipari, G., & Szabo, A. (1980) *Biophys. J. 30*, 489.

Lyamichev, V. I., Mirkin, S. M., Frank-Kamenetskii, M. D., & Cantor, C. R. (1988) *Nucleic Acids Res. 16*, 2165.

Mhaskar, D. N., & Goodman, M. F. (1984) *J. Biol. Chem. 259*, 11713.

Millar, D. P., & Sowers, L. C. (1990) *Proc. SPIE-Int. Soc. Opt. Eng. 1204*, 656.

Mirkin, S. N., Lyamichev, V. I., Drushlyak, K. N., Dobrynin, V. N., Fillipov, S. A., & Frank-Kamenetskii, M. D. (1987) *Nature 330*, 495.

Modrich, P. (1987) *Annu. Rev. Biochem. 56*, 435.

Morgan, J. P., & Daniels, M. (1980) *Photochem. Photobiol. 32*, 101.

Moser, H., & Dervan, P. B. (1987) *Science 238*, 645.

Nordlund, T. M., Andersson, S., Nilsson, L., Rigler, R., Graslund, A., & McLaughlin, L. W. (1989) *Biochemistry 28*, 9095.

Patel, D. J., Kozlowski, S. A., Ikuta, S., & Itakura, K. (1984) *Biochemistry 23*, 3207.

Povsic, T. J., & Dervan, P. B. (1989) *J. Am. Chem. Soc. 111*, 3059.

Rajagopal, P., & Feigon, J. (1989) *Nature 339*, 637.

Sowers, L. C., Fazakerley, G. V., Eritja, R., Kaplan, B. E., & Goodman, M. F. (1986) *Proc. Natl. Acad. Sci. U.S.A. 83*, 5434.

Sowers, L. C., Eritja, R., Chen, F. M., Khwaja, T., Kaplan, B. E., Goodman, M. F., & Fazakerley, G. V. (1989) *Biochem. Biophys. Res. Commun. 165*, 89.

Wagner, R., Dohet, C., Jones, M., Doutriaux, M.-P., & Radman, M. (1984) *Cold Spring Harbor Symp. Quant. Biol. 49*, 611.

Watanabe, S. M., & Goodman, M. F. (1981) *Proc. Natl. Acad. Sci. U.S.A. 78*, 2864.

White, J. H., Lusnak, K., & Fogel, S. (1985) *Nature 315*, 350.